Analysis of orbital angular momentum laser beams for applications in underwater communication

Joseph Brugger, Charles Nelson

Joseph Brugger, Charles Nelson, "Analysis of orbital angular momentum laser beams for applications in underwater communication," Proc. SPIE 10631, Ocean Sensing and Monitoring X, 106310S (25 May 2018); doi: 10.1117/12.2309865

SPIE.

Event: SPIE Defense + Security, 2018, Orlando, Florida, United States

Analysis of Orbital Angular Momentum Laser Beams for Applications in Underwater Communication

Joseph Brugger*, Charles Nelson,
United States Naval Academy, Electrical and Computer Engineering Department
121 Blake Road, Annapolis, MD, USA 21402

ABSTRACT

Underwater communications present a challenge in the US Naval Undersea Community. During underwater operations, command and control requires effective communication on both a tactical (short-range) and strategic (long-range) level. One approach to address this issue would be the use of an optical beam to transmit underwater. This paper evaluates the use of an Orbital Angular Momentum (OAM) beam and their effectiveness in underwater transmissions as compared to a Gaussian beam. The normalized variance, or scintillation index is used as the metric for comparison. Additionally, an in-laboratory underwater turbulence emulator is used to generate and control various environmental parameters to include varying levels of salinity as well as temperature gradients. The goal of the emulation is to be able to simulate some of the scaled effects of various environments in order to better predict and gain intuition and understanding of the performance of an optical system in various environments. Results provided evaluate efficiency as a function of environmental conditions and scintillation index. Transmission in the 532 nm band is analyzed.

Keywords: Gaussian, OAM, scintillation, emulation, underwater, optical communication

1. INTRODUCTION

Lasers exhibit properties of both waves and particles in order to create monochromatic light; that is both directional and coherent. There are two main propagations of lasers that will be researched, Orbital Angular Momentum (OAM) and Gaussian. Gaussian laser beams are directed energy beams that propagate in a straight line, while OAM beams propagate in a helical manner. The OAM beams create a "donut"-like shape when viewed from a direct angle. It is important to note that as the modulation index of the beam increase, the output profile of the beam generates a tighter spiral. While there are many papers on OAM propagation, ref. 1 demonstrated that as the magnitude of OAM increased, the relative amplitude of the received signal also increased. This means that the amount of scattering and dispersion decreases since more light is collected as the OAM magnitude increases.[1]

Ref. 2 talks about the ability of OAM laser beams to transmit information. In this paper, Wang and Willner establish the ability of OAM to multiplex in order to encode signal and data information, but also the ability of higher order OAM beams to further boost spectral efficiency and transmission capacity.[2] These references support the notion that higher order OAM beams transmit more effectively than Gaussian through a medium. This project seeks to validate these concepts in terms of scintillation index as opposed to bit rate and attenuation factors. Ref. 3 address the idea that high levels of induced scattering will negatively impact the transmission of optical beams underwater. In this paper, Dr. Cochenour also determined that there was no significant modulation loss as the scattering and turbidity of the water medium increased. This is important because it proposes the idea that output modulation level will remain relatively constant independent of various water factors.[3] Ref. 4 address the idea that optical links are a viable option for high bandwidth wireless links underwater. Dr. Cochenour determined that the idea range for these communications would be less than 100m. This would accurately allow for minimal scattering effects as well as no loss of modulation.[4] These two papers address the consistency of OAM beams to maintain their indices as well as narrow down the range at which optical beams can be effective. Further testing at higher ranges is essential to determining the usability of optical beams for long range communications underwater.

*Joseph A. Brugger; audi21.ab@gmail.com

Ocean Sensing and Monitoring X, edited by Weilin (Will) Hou, Robert A. Arnone, Proc. of SPIE
Vol. 10631, 106310S · © 2018 SPIE · CCC code: 0277-786X/18/$18 · doi: 10.1117/12.2309865

In past years, students at the Naval Academy have looked at statistical probabilities and models surrounding the concept of underwater beam propagation. For example, previous work by Bernotas et al explored the use of Weibull and exponentiated Weibull probability density functions in data analysis to provide the most accurate mathematical models to model the behavior of laser propagation through water.[5] This project builds off of this work through extensive experimentation involving firing in different environments, and with different types of OAM laser optical transmission. Additional studies at the Naval Academy focused on first determining scintillation indices and then comparing the output values to determine if there is significant deviation between the two beams variance of propagation.[6] Scintillation index is a measure of the variance of the intensity of the received signal as compared to the transmitted signal.

This project explores the use of an in-lab emulator to model the behavior of various environments around the world. The emulator uses variables of temperature and salinity in order to model and map the behavior of optical beam transmission in different surroundings.

The first variable considered was temperature. Temperature concerns both surface temperature and depth. According to the National Oceanographic and Atmospheric Administration there is a wide range varying surface temperatures around the world. Changing temperatures are important because as temperature changes, the refractive index of water also changes.[7] Changing refractive indices have been shown to alter the propagation of optical beams. Another aspect of temperature is the temperature gradients or levels that form as depth increases. The key component of gradients are thermoclines. Thermoclines form when there are distinctive differences in temperature between various bands or layers of water. Thermoclines would affect transmission by acting like a barrier and cause refraction to occur.[8] It is important to note that while the surface and deep-water layers are fairly constant temperature, the thermocline layer is a region of rapid temperature change.

The next water property considered was salinity. Salinity is the measure of the salt concentration in a water body. It has been determined to have significant effects on the transmission of optical beams by altering the spreading behavior of the beam. As salinity increases, spreading of the beam will also increase. Similar to temperature, salinity can also experience a layer differential which will cause issues with refraction and reflection of optical beams. The zone is referred to as the halocline layer. Halocline refers to multiple layers of water having a vastly different salt concentrations.[9] Halocline is important because these layers can stretch from single meters to 10's of meters in height. The fluctuation means that any beam transmission will likely be oscillating between layers.

2. DESIGN PROCESS

The basic emulator setup consists of a laser, phase plate, water tank, neutral filter, and camera. These various components are cascaded in a series shown in Fig. 1.

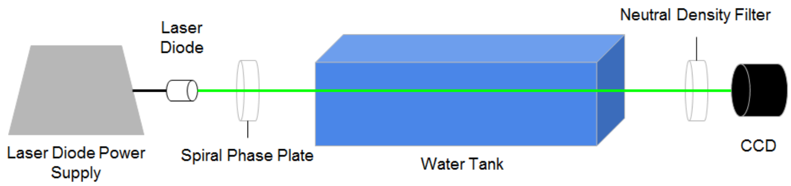

Figure 1. Basic Schematic of Testing Apparatus[5]

2.1 Design of Tank

The tank shown in Fig. 2, was the main testing apparatus in this project. The tank is one meter long and has both heating coils and thermocouples spaced within. The four heating coils were evenly spaced 20cm apart horizontally. This was done to ensure even and equal heat distribution across the entire tank. The thermocouples or temperature sensors were placed horizontally at the same intervals as the heating coils. It was also determined through testing, that a vertical temperature differential existed. In order to measure the vertical temperature differential, more thermocouples were added. In the final design, twelve thermocouples were used and stacked in groups of three, vertically placed 2cm apart and horizontally 20 cm apart, same as the heating coils.

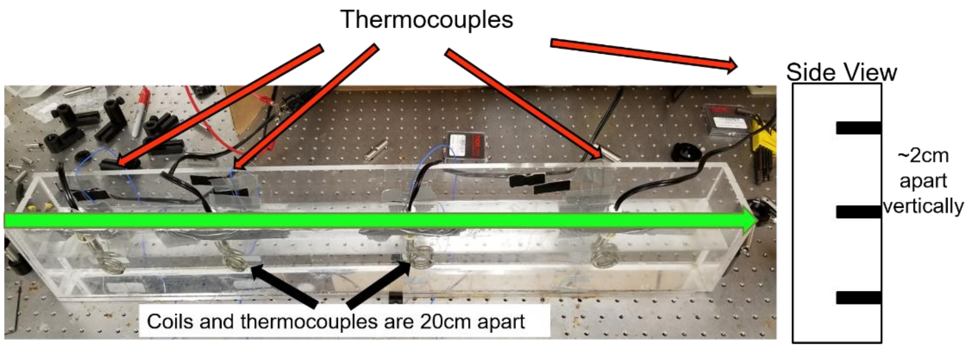

Figure 2. Thermocouple and Heating Coil Spacing

2.2 Water Conditions

The next step in the design process was determining the proper temperatures and salinity concentrations for experimentation. The temperatures of 21°C, 23°C, and 28°C were chosen for testing, since a majority of the surface temperatures around the world fall within this range. These temperatures would be reached by connecting the heating coils to a controlled voltage source in order to maintain constant temperature of the coils for the duration of testing. It was later determined that the vertical temperature gradient could be measured as well and would remain constant for the length of testing. This validation was determined by measuring the consistency of water temperature over the course of a 30 second test. If the water temperatures remained constant, then the model could be accurately used for further emulation of various environments. The temperature tested was a three degree vertical temperature differential.

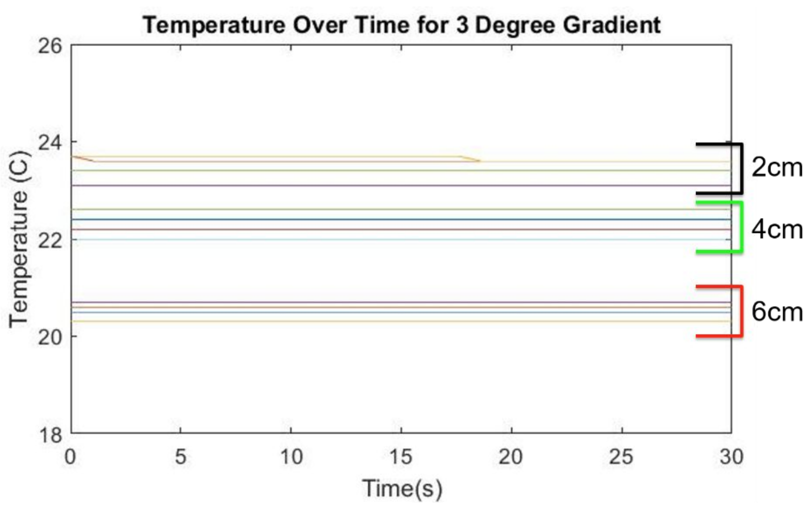

Figure 3. Temperature Plot for 3 Degree Gradient with Depths Identified

Figure 3 represents all 12 thermocouple sensors and their respective depths from the surface. It is important to note the consistency of the temperatures at each depth over the testing period.

In terms of salinity, two salt concentrations were used. The models considered were brackish and ocean water. Brackish water is made up of approximately 20000 ppm of salt. This would represent water bodies such as the Severn River and other small water bodies that lie along the coast and have the potential to interact to the oceans. Ocean water consists of approximately 35000 ppm of salt. These concentrations would allow for modeling of salt's effects on the propagation of beams. These concentrations were made with over the counter table salt.

2.3 Laser Setup

A 532nm wavelength laser was used for testing. The beam was first sent through a phase plate which would either maintain the Gaussian shape of the beam or modulate it to fit one of the OAM profiles. 8-order and 16-order OAM phase plates were used to provide the optical vortexing in order to generate the OAM profile. The phase plate generates a spiral based on the angle of spin within the plate.[10]

3. DATA COLLECTION AND ANALYSIS

The main sources of data collection were timed series outputs that were measured and tracked by the CCD camera. The CCD camera generated a 30 second time series spread of 1024 x 1024 images. The camera was operating with a frame rate of 14.97 FPS and an exposure time of 66.52 ms. For each variable tested, at each OAM and Gaussian modulation level, five tests were run and then averaged to provide results. In order to track the scintillation index across the time series calculations of 30 seconds, the analysis portion first consisted of locating the pixel with the highest power and then calculating an average of the pixels around it in a 5x5 square. To account for background noise in the intensity readings, a baseline with zero laser propagation was taken and subtracted from the recorded output values. In order to prevent oversaturation of the camera, neutral density(ND) filters of a total value of 4.5 were implemented.

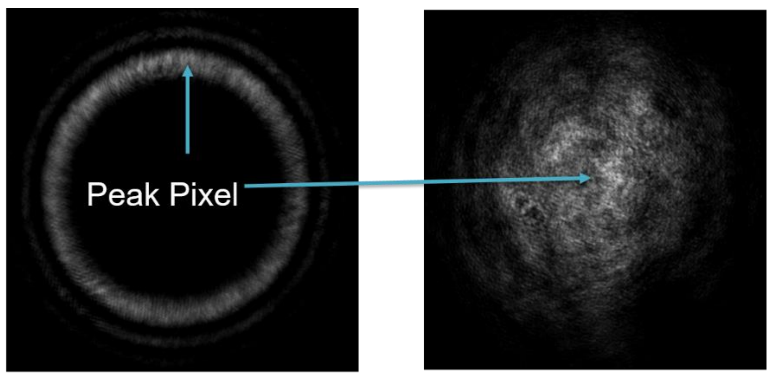

a) 16 Order OAM Output Profile b) Gaussian OAM Output Profile

Figure 4. OAM 16 Order Profile (Left) and Gaussian Profile (Right) Peak Pixel Location

Figure 4 depicts a potential location for the peak pixel of both a Gaussian and OAM 16 order output profile that would be tracked by the camera over a representative time series as shown in Fig. 5.

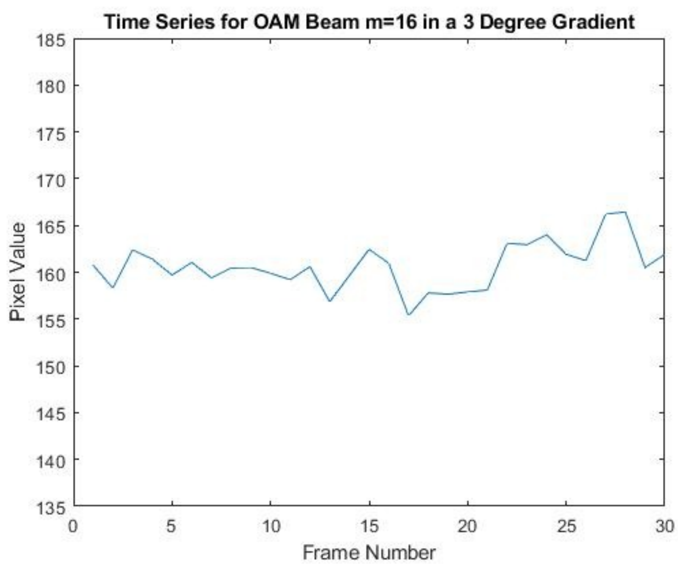

Figure 5. OAM 16 Output Time Series Plot for a 3 Degree Temperature Gradient

3.1 Single Region Analysis

The main statistic being tracked throughout this project is scintillation index. This measurement can help determine the effectiveness of the signal's wavelengths and energy staying together as it propagates through a medium. The ideal value for this statistic is 0, representing a perfect transmission with no loss. The equation for calculating scintillation index is

$$\sigma^2 = \frac{<I^2>-<I>^2}{<I^2>} = \frac{<I^2>}{<I>^2} - 1 \tag{1}$$

This scintillation index provides an accurate representation of the ability of the specific beam to maintain its coherence. The variables tested were the temperatures and salinity concentrations previously stated, in addition to a 3 degree vertical temperature gradient. The overall average scintillation values for the respective variables are shown Fig. 6. Each data point represents an average of 5 trial runs with the entire plot representing 90 total trials.

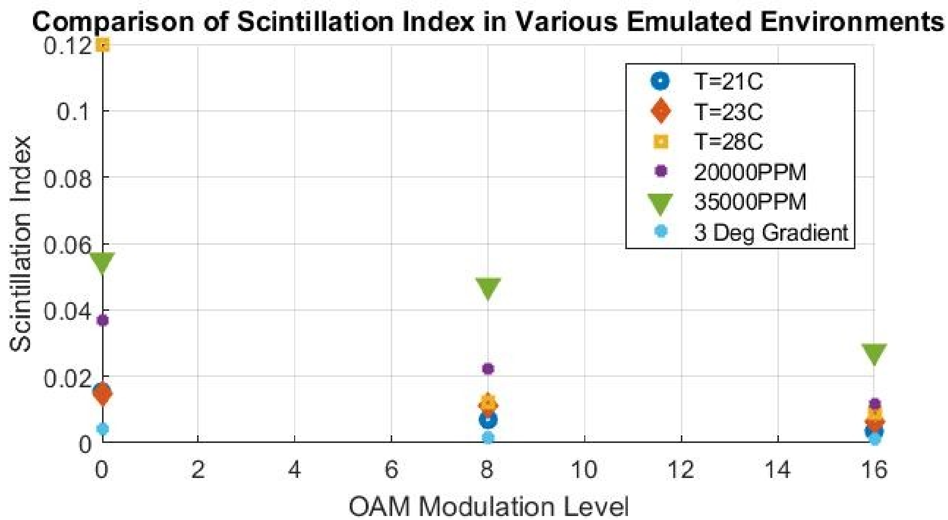

Figure 6. Scintillation Index for Various Variables

Figure 6 highly suggests that there is variation between the Gaussian (0 Modulation Level) and OAM modulation levels (Modulation Levels of 8 and 16) in terms of the scintillation index as the beams pass through various mediums. The most extreme differential appears to be with the 28°C data as it appears that the high temperature strongly affects the Gaussian beam. The least extreme differential appears to be the 35000 ppm salt concentration which could be the result of massive diffraction as the beam spreading would be greatest with the highest amount of substance in the water. In order to quantify the difference between these values, a percent reduction table (Table 1) was calculated, in addition to statistical analysis in the form of a T-test where p-values (Table 2) were generated.

Table 1. Percent Reduction of Scintillation Index

	G vs m=8	G vs m=16	8 vs 16
21°C	55%	77%	50%
23°C	24%	56%	42%
28°C	90%	92%	25%
20000ppm	39%	69%	48%
35000ppm	14%	50%	42%
3°C Gradient	60%	79%	48%

Table 2. T-test p-Values for Scintillation Index

	G vs m=8	G vs m=16	8 vs 16
21°C	1.71E-05	7.63E-10	8.90718E-05
23°C	0.004751	1.76E-05	2.47842E-05
28°C	0.000196	0.000182	0.007215942
20000ppm	0.001018	3.76E-06	0.000732216
35000ppm	0.009992	1.82E-06	4.70728E-05
3°C Gradient	6.48E-05	0.000106	0.003899859

These tables support the claim that the difference in OAM modulation level appears to have a significant variation on the scintillation index. This conclusion can be drawn from the small p-Values and the large percent reduction between Gaussian and OAM and even within the OAM modulation levels.

3.2 Multi-Region Analysis

Further analysis was performed in order to determine if a multi-region analysis would demonstrate better performance than the single region analysis, demonstrated in the previous section. Scintillation indices were explored in four quadrants (Fig. 7a) or regions of 1 pixel, 9 pixels, and 25 pixels. The regional analysis was initially performed on both Gaussian and OAM output profiles but the Gaussian was switched to the center (Fig.7b) as the points were naturally localizing on the center of the beam shape.

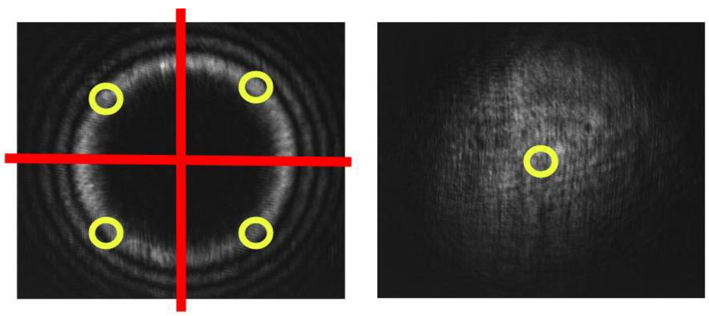

a) OAM 8 Modulation Divided into Quadrants b) Gaussian Centered on Highest Power Output

Figure 7. Regional/Quadrant Analysis for Pixel Selection

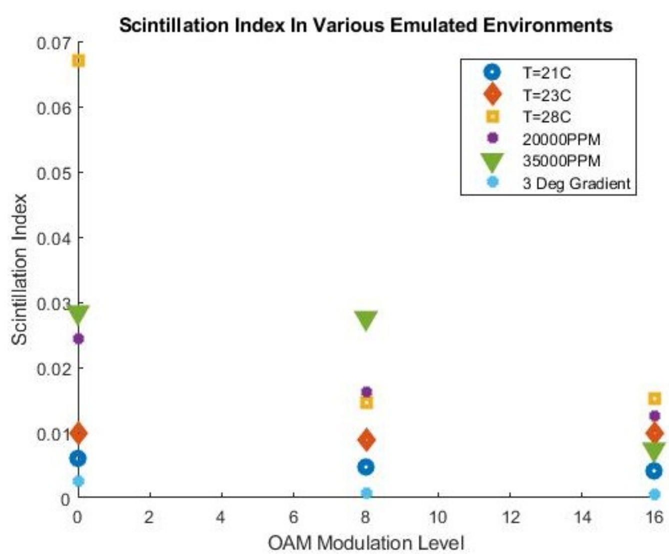

Figure 8. Regional/Quadrant Analysis for 1 Pixel Selection

Table 3. T-test p-Values Regional/Quadrant Analysis for 1 Pixel Selection

	G vs m=8	G vs m=16	m=8 vs m=16
21°C	0.008793	0.000681	0.115657462
23°C	0.372389	0.49699	0.327064037
28°C	2.88E-06	6.13E-06	0.404970888
20000ppm	0.00837	0.00219	0.038369986
35000ppm	0.331852	1.78E-05	5.41438E-05
3°C Gradient	0.046056	0.029525	0.024009333

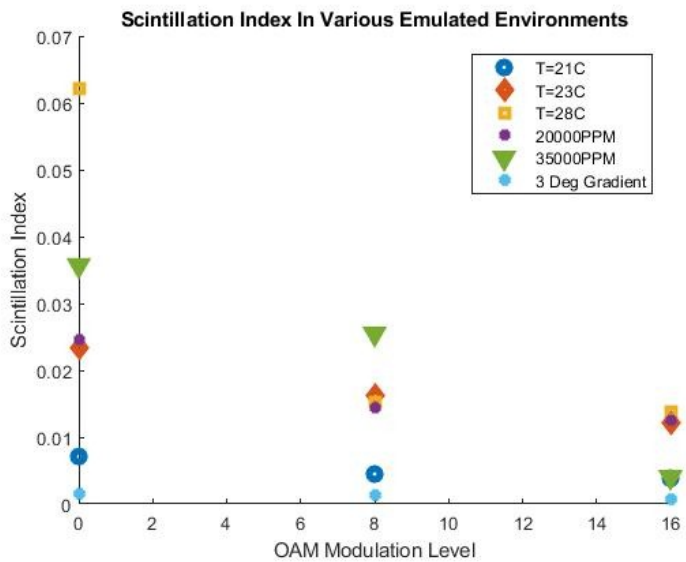

Figure 9. Regional/Quadrant Analysis for 9 Pixel Selection

Table 4. T-test p-Values Regional/Quadrant Analysis for 9 Pixel Selection

	G vs m=8	G vs m=16	m=8 vs m=16
21°C	3.78E-05	3.01E-06	0.039839988
23°C	0.005511	0.001089	3.98635E-06
28°C	9.23E-10	3.96E-14	0.029119365
20000ppm	6.58E-05	4.06E-05	0.00025334
35000ppm	8.11E-06	1.78E-07	3.21696E-08
3°C Gradient	0.099975	0.001646	0.001634741

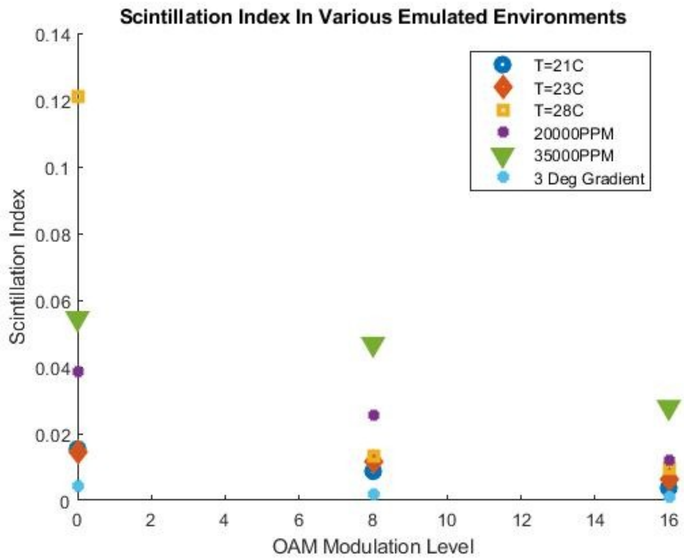

Figure 10. Regional/Quadrant Analysis for 25 Pixel Selection

Table 5. T-test p-Values Regional/Quadrant Analysis for 25 Pixel Selection

	G vs m=8	G vs m=16	m=8 vs m=16
21°C	1.71E-05	7.63E-10	8.90718E-05
23°C	0.004751	1.76E-05	2.47842E-05
28°C	0.000196	0.000182	0.007215942
20000ppm	0.001018	3.76E-06	0.000732216
35000ppm	0.009992	1.82E-06	4.70728E-05
3°C Gradient	6.48E-05	0.000106	0.003899859

Figures 8-10 highly support the idea of variation between the Gaussian and OAM modulation levels in terms of the scintillation index as the beams pass through various mediums. Throughout the regional analysis it appears that as OAM modulation index increases, the scintillation index decreases. This is apparent for the 9-Pixel and 25-Pixel Region Analysis.' Tables 4 and 5 of p-Values for both of these tests affirm this statement as the values are all less than 0.05, highly suggesting that significant variation is occurring between the variables of OAM index. In terms of the 1-Pixel analysis it appears that there was not significant variation between the various OAM indices according to Table 3. Within Table 3 the overall p-Values are inconsistent and very sporadic. It was interpolated that 1-Pixel captures are too variable, even with the averaging of the four regions, to gather enough data in order to make accurate predictions about the trends or correlations.

4. CONCLUSIONS

At this point, based on the high amount of experimental testing, it appears that there is a significant variation between the scintillation indices of the Gaussian and OAM order laser beams. This is based upon the p-values which all fall much less than the standard cutoff of 0.05. This highly suggest that the variation seen in this project is due to the OAM charge as opposed to some external environmental factor. This trend is seen across both the single region analysis and the multi-region analysis. It is recommended that future testing use the 9-Pixel regional analysis to collect and interpret the data. However, more testing is required to affirm this statement. More testing shall be performed over longer ranges and with more factors in order to accurately gauge the overall behavior in all situations. When looking at the temperature differential, it appears that for the course of a time series plot, the temperature remains constant at each of the levels as tracked by the thermocouples. This means that the emulator is stable and controllable and can be used to model further environments accurately.

Future studies will consist of testing further temperatures of water but also focusing on the temperature gradients in order to induce potential changes. There will be field testing, and more environmental conditions to be tested. These conditions can consist of sediment testing and more salinity concentrations. There is also the potential to assign probability density functions for testing.

REFERENCES

[1] Brandon Cochenour, Kaitlyn Morgan, Keith Miller, Eric Johnson, Kaitlin Dunn, and Linda Mullen, "Propagation of modulated optical beams carrying orbital angular momentum in turbid water," Appl. Opt. 55, C34-C38 (2016)

[2] J. Wang and A. E. Willner, "Using orbital angular momentum modes for optical transmission," OFC 2014, San Francisco, CA, 2014, pp. 1-3.

[3] B. Cochenour, L. Mullen, A. Laux and T. Curran, "Effects of Multiple Scattering on the Implementation of an Underwater Wireless Optical Communications Link," OCEANS 2006, Boston, MA, 2006, pp. 1-6.

[4] B. Cochenour, L. Mullen and A. Laux, "Spatial and temporal dispersion in high bandwidth underwater laser communication links," MILCOM 2008 - 2008 IEEE Military Communications Conference, San Diego, CA, 2008, pp. 1-7.

[5] M. Bernotas, and C. Nelson, "Probability density function analysis for optimization of underwater optical communications systems." OCEANS'15 MTS/IEEE Washington (2015).

[6] Jung, Daniel "Underwater Propagation of Orbital Angular Momentum Beam", EE496 Independent Research Course Final Report, USNA, May 2016.

[7] "Chart of Ocean Temperature", NOAA, http://www.ospo.noaa.gov/Products/ocean/sst/contour/index.html, Accessed 8 March 2017

[8] "Thermocline Layer", Living Oceans Foundation, https://www.livingoceansfoundation.org/assets/2015/04/ Figure-7-5.jpg, Accessed 8 March 2017

[9] "Halocline", Slideshare, https://image.slidesharecdn.com/pressuredensitynotes1112-111024083700-phpapp02/95/temperature-salinity-density-notes-1112-6-728.jpg?cb=1319445476, Accessed 8 March 2017.

[10] "Phase Plate", Computational Nonlinear & Quantum Optics Group, http://cnqo.phys.strath.ac.uk/wp-content/uploads/2012/03/phase-plate.jpg, Accessed 10 March 2017.

[11] Ladanyi, L. "Effects of random temperature and pressure influence on the single-channel optical transmission system", http://ieeexplore.ieee.org/xpls/icp.jsp?arnumber=6705203, accessed 12 March 2017

[12] "Twisted Light could dramatically Boost Data Rates", IEEE Spectrum, http://spectrum.ieee.org/telecom/ wireless/twisted-light-could-dramatically-boost-data-rates, accessed January 2017.